Biolistics-mediated transformation of hornworts and its application to study pyrenoid protein localization

Running title: Biolistics-mediated transformation of hornworts

Declan J. Lafferty[1], Tanner A. Robison[1,2], Andika Gunadi[3], Laura H. Gunn[2,4], Joyce Van Eck[1,5], Fay-Wei Li[1,2,*]

[1]Boyce Thompson Institute, Ithaca, NY 14853

[2]Plant Biology Section, School of Integrative Plant Science, Cornell University, Ithaca, NY 14853

[3]J.R. Simplot Company, Boise, ID 83707

[4]Plant Department of Cell and Molecular Biology, Uppsala University, S-751 24 Uppsala, Sweden

[5]Plant Breeding and Genetics Section, School of Integrative Plant Science, Cornell University, Ithaca, NY 14853

*Author of correspondence: Fay-Wei Li (fl329@cornell.edu)

Email addresses

Declan J. Lafferty: djl346@cornell.edu

Tanner A. Robison: tar226@cornell.edu

Andika Gunadi: andika.gunadi@simplot.com

Laura H. Gunn: lhg42@cornell.edu

Joyce Van Eck: jv27@cornell.edu

Date of submission: 10.23.2023

Number of tables and figures: 5 figures and 1 table

Word count: 3012

Supplemental data: 5 figures and 1 table

25 **Highlight**

26 We developed a new transformation method for hornworts, a lineage of understudied bryophytes, and
27 demonstrated its effectiveness in studying subcellular localization of proteins involved in pyrenoid-based
28 CO_2-concentrating mechanism.

29

30 **Abstract**

31 Hornworts are a deeply diverged lineage of bryophytes that are sister to mosses and liverworts.
32 Hornworts have an array of unique features that can be leveraged to illuminate not only the early
33 evolution of land plants, but also alternative paths for nitrogen and carbon assimilation via cyanobacterial
34 symbiosis and a pyrenoid-based CO_2-concentrating mechanism (CCM), respectively. Despite this,
35 hornworts are one of the few plant lineages with limited available genetic tools. Here we report an
36 efficient biolistics method for generating transient-expression and stable transgenic lines in the model
37 hornwort, *Anthoceros agrestis*. An average of 569 (± 268) cells showed transient expression per
38 bombardment, with green fluorescent protein expression observed within 48 hours. A total of 81 stably
39 transformed lines were recovered across three separate experiments, averaging six lines per
40 bombardment. We followed the same method to transiently transform nine additional hornwort species,
41 and obtained stable transformants from one. This method was further used to verify the localization of
42 Rubisco and Rubisco activase in pyrenoids, which are central proteins for CCM function. Together, our
43 biolistics approach offers key advantages over existing methods as it enables rapid transient expression
44 and can be applied to widely diverse hornwort species.

45

46 **Keywords:** *Anthoceros agrestis*, biolistics, bryophyte, CO_2-concentrating mechanism, fluorescent protein
47 tagging, gene gun, hornwort, pyrenoid

48

49 **Abbreviations:** BUSCO (Benchmarking Universal Single-Copy Orthologue), CCM (CO_2-concentrating
50 mechanism), Ef1α (Elongation factor 1 alpha), GFP (green fluorescent protein), HPT (hygromycin
51 phosphorylase), RbcS (Rubisco small subunit), RCA (Rubisco activase), Rubisco (ribulose-1,5-bisphosphate
52 carboxylase/oxygenase),

53

54 **Introduction**

55 Hornworts are a unique group of bryophytes that exhibit distinct traits among land plants. Evolutionarily,
56 hornworts diverged from the closest extant clade, setaphytes (mosses and liverworts), over 480 million
57 years ago (Morris et al., 2018). Many of hornworts' developmental, anatomical, and physiological features
58 are not found in other plant lineages. As such, hornworts are of paramount importance to retrace plant
59 evolutionary history (Li et al., 2020; Frangedakis et al., 2021a; Frangedakis et al., 2021b).

60 Hornworts have evolved unconventional ways to source nitrogen and carbon. For nitrogen, all hornwort
61 species are known to engage in a symbiotic relationship with nitrogen-fixing cyanobacteria (Meeks, 1998;
62 Nelson et al., 2021). Symbiotic cyanobacteria are hosted inside specialized slime cavities in the hornwort
63 thallus, where they differentiate into heterocysts, a cell type dedicated to nitrogen fixation. While several
64 hornwort genes have been recently identified that might be involved in symbiosis regulation or
65 maintenance (Li et al., 2020; Chatterjee et al., 2022), they have not been functionally characterized.

66 For carbon capture, hornworts are the only land plants that evolved a pyrenoid-based CO_2-concentrating
67 mechanism (CCM). In this case, the CO_2-fixing enzyme, ribulose-1,5-bisphosphate carboxylase/oxygenase
68 (Rubisco), is compartmentalized inside pyrenoids, which are special chloroplast structures sandwiched by
69 thylakoids (Vaughn et al., 1992). Through the coordinated actions of bicarbonate transporters and
70 carbonic anhydrases, CO_2 is concentrated within pyrenoids thereby boosting the efficiency of Rubisco (Li
71 et al., 2017; He et al., 2023). Interestingly, pyrenoids (and the associated CCM) have been repeatedly
72 gained and lost during hornwort evolution (Villarreal & Renner, 2012), providing unique evolutionary
73 replications for examining the underlying genetic mechanisms. It has been hypothesized that engineering
74 a biophysical CCM into crop plants could enhance photosynthetic efficiency (Adler et al., 2022), but
75 attempts to transfer algal pyrenoid-based CCM are challenged by the incompatibility between land plant
76 Rubisco and algal pyrenoid components (Meyer et al., 2016; Atkinson et al., 2020). On the other hand,
77 hornwort Rubisco and chloroplasts are both evolutionarily and structurally similar to those in crop plants,
78 providing a CCM that may be more readily engineered into crops. Currently, none of the genetic
79 components of hornwort pyrenoid structure and development have been identified, outside of Rubisco.

80 *Anthoceros agrestis* has recently emerged as a potential model hornwort species, with a sequenced
81 genome and an optimized tissue culture growth medium (Szövényi et al., 2015; Li et al., 2020; Gunadi et
82 al., 2022). Its life cycle is dominated by a haploid gametophyte stage, making it an ideal target for genetic
83 engineering. However, the lack of transformation tools has hampered the progress of functional

84 genomics in hornworts. Recently, an *Agrobacterium*-mediated transformation method was reported for
85 *A. agrestis* and has been successfully used for a number of hornwort species (Frangedakis et al., 2021b;
86 Waller et al., 2023). Transient transformation of hornwort protoplasts has also been reported (Neubauer
87 et al., 2022), although thalli regeneration from protoplasts has not been possible. The biolistics method,
88 also known as particle bombardment or gene gun technology, is another powerful tool used for genetic
89 engineering (Sanford et al., 1987) and that has not been explored for hornworts. This method involves the
90 introduction of microscopic particles coated with DNA into plant cells.

91 Biolistics has a number of advantages over other transformation methods. First, it is relatively simple and
92 requires less technical expertise. The preparation time for biolistics is relatively fast, taking less than a
93 couple of hours for particle preparation and subsequent transformation. *Agrobacterium*-mediated
94 methods involve the use of live bacteria and co-cultivation steps, and protoplast transformation requires
95 cell wall digestion, all of which can be difficult to optimize (Lacroix & Citovsky, 2020). Second, biolistics
96 can deliver a wider range of cargoes into plant cells including plasmid DNA, linearized DNA (such as PCR
97 products), RNA, ribonucleoproteins, and proteins (Fu et al., 2000; Martin-Ortigosa & Wang., 2014;
98 Svitashev et al., 2016; Zhang et al., 2016). Finally, biolistics can be used to transform plastids (Boynton et
99 al., 1988; Svab et al., 1990), which is crucial to study the genes involved in pyrenoid function. Conversely,
100 the downsides of the biolistics method include the possibility to cause severe cellular damage and the
101 method may require expensive supplies and equipment. Reports have also shown a higher number of
102 integrated gene copies when compared with *Agrobacterium*-mediated transformation, potentially
103 causing genetic instability and gene silencing (Kohli et al., 2003). The extent of these impacts, however,
104 has not yet been explored in hornworts.

105 In this study, we describe the development of a biolistics transformation method for hornworts,
106 demonstrating both transient and stable transformation of *A. agrestis* and *A. fusiformis*, as well as
107 transient transformation of nine other species across the hornwort tree of life. These transformable
108 species share the most recent common ancestor almost 300 million years ago, before the origin of
109 flowering plants. Using our optimized method, we were able to observe transient expression of the green
110 fluorescent protein (GFP) reporter gene within two days of transformation, and recover stable transgenic
111 lines after 8-10 weeks. Importantly, we applied this method to examine the subcellular localization of
112 Rubisco and Rubisco activase, both of which are key elements in CCMs, which represents the first gene
113 functional study in hornworts, and allows for comparative research across bryophytes and vascular plants.

114

115 **Materials and Methods**

116 ***Plant tissue preparation***

117 *Anthoceros agrestis* cultures were grown axenically on AG medium supplemented with 0.2% sucrose at
118 22°C under a 16/8 h light/dark cycle with 6-25 µmol/m²/s light intensity provided by Ecolux XL Starcoat
119 F32T8 XL SP30 ECO paired with F32T8 XL SP41 ECO fluorescence bulbs (General Electric, USA) as described
120 in Gunadi et al. (2022). Thallus tissue (haploid) was prepared for transformation by placing 3-6 g (fresh
121 weight) of tissue in a 50 mL Falcon tube containing 30 mL of sterile deionized water, containing 30 µL of
122 300 mg/mL timentin (final concentration of 300 mg/L) (T-104-25, Goldbio, USA), followed by
123 homogenization with a T18 digital ULTRA TURRAX homogenizer (IKA, Germany) for 5 s at 4000 rpm. The
124 tissue was filtered using a 100 µM cell strainer (C4100, MTC Bio, USA) and washed with 50 mL sterile
125 deionized water. Approximately 200 mg of tissue was plated on AG medium, supplemented with 2%
126 sucrose. Tissue was spread as thinly as possible in a 2.5 cm circle using a Nunc cell scraper (ThermoFisher
127 Scientific, USA). The plates were left open for 10 min to remove excess moisture. Tissue was allowed to
128 recover for 7 days before transformation. These procedures were done in a laminar flow hood.

129

130 ***DNA construct preparation***

131 Constructs were designed using the OpenPlant toolkit (Sauret-Güeto et al., 2020). The Aa049 construct
132 was assembled using the following L0 parts: Native *A. agrestis Elongation factor 1 alpha* (*Ef1α*) promoter,
133 OP_049 35S promoter, OP-020 *hygromycin phosphotransferase* (*hpt)*, OP-023 *eGFP*, OP_037 *CTAG_Lti6b*,
134 OP-053 *NoS* terminator. Vector ligations and *E. coli* transformation were performed as described in
135 Frangedakis et al. (2021b). To obtain high concentrations of plasmid DNA, 100 ml of *E. coli* culture was
136 grown overnight at 37°C. The plasmid DNA was extracted using the PureYield™ Plasmid Midiprep System
137 (A2492, Promega, USA), followed by vacuum concentration in a SpeedVac Concentrator (Thermofisher
138 Scientific, USA) to obtain DNA concentrations of 1 µg/µL.

139

140 ***Gold particle preparation***

141 To prepare for 10 separate bombardments, a total of 20 µL of 1 µg/µL plasmid DNA was combined with
142 50 µL of gold microparticles (1 µm, 50 mg/ml, suspended in 50% (v/v) sterile glycerol) (#1652263, Bio-Rad,
143 USA), 100 µL 2.5 M $CaCl_2$ and 40 µL 0.1 M spermidine (S0266, Sigma-Aldrich, USA), under constant

144 vortexing. The DNA/gold mixture was vortexed for 1 min before being pelleted by centrifugation at 3500
145 x g for 8 s. The supernatant was removed and 180 µL of 70% (v/v) ethanol was added and vortexed for 1
146 min. The DNA/gold mixture was centrifuged again at 3500 x g for 8 s. The supernatant was removed and
147 200 µL of 100% ethanol were added and vortexed for 1 min, followed by another centrifugation step and
148 the removal of 135 µL of supernatant. The DNA/gold mixture was resuspended in a Branson 2510
149 Ultrasonic Cleaner and 5 µL was spread onto each sterilized macrocarrier (#1652335, Bio-Rad, USA) and
150 left to dry for 30 min.

151

152 ***Biolistics transformation***

153 Biolistics was performed using the Particle Delivery System PDS-1000/He (#1652257, Bio-Rad, USA).
154 Thallus tissue was bombarded with a target distance of 14 cm, under a vacuum of 28 inHg. The burst
155 pressure was generated using a 450 psi rupture disk (#1652326, Bio-Rad, USA). The macrocarrier and
156 rupture disc were retained using a stopping screen (#1652257, Bio-Rad, USA). The tissue was left to
157 recover for 7 days.

158

159 ***Imaging and quantification of transient transformation efficiency***

160 Transient transformation efficiency was estimated using a pipeline developed in CellProfiler (v4.2.5)
161 (Stirling et al., 2021). Fluorescent images of transformed tissues were taken 3 days post bombardment,
162 using a GPF filter on a Leica M205 stereomicroscope at a magnitude of 10 mm x 7.5 mm. Nine images
163 were taken to encompass all tissue used for transformation. The exposure time was set between 10 – 12
164 s, depending on transient GFP fluorescent intensity, and was kept constant for all images within an
165 experiment. The default pipeline parameters were used with adjustments made to cell diameter (between
166 6- and 30-pixel units in diameter) and object intensity (green intensity between 0.1 and 0.9). Red signal
167 represents cells expressing GFP and blue signals are objects classified by CellProfiler that are not
168 expressing GFP; these may be artifacts or untransformed cells/tissue. The pipeline can be found on
169 Figshare (10.6084/m9.figshare.24243559). The number of transients in each photo was combined to show
170 the total transients in each replicate.

171

172

173 ***Regeneration of stably transformed lines***

174 To regenerate stably transformed lines, tissue from all replicates was pooled and homogenized (as
175 described above) 7 days post bombardment. The homogenized tissues were collected using a 100 µM cell
176 strainer, washed with sterile water, and thinly spread on 70 mm diameter Whatman filter paper
177 (WHA1001070, Sigma-Aldrich, USA) overlain on solid AG medium supplemented with 0.2% sucrose. The
178 number of plates prepared corresponds to the number of replicates pooled. This tissue was left to recover
179 for 3 days before transfer to AG medium supplemented with 0.2% sucrose and 10 mg/L hygromycin
180 (#10687010; Invitrogen, USA), by moving the filter paper containing the tissue. After 4 weeks the tissue
181 was transferred again to fresh AG medium supplemented with 0.2% sucrose and 10 mg/L hygromycin.
182 Stably transformed thallus tissue is visible within 8-10 weeks of transformation. Images were taken on a
183 Leica M205 stereomicroscope and a Leica TCS SP5 Laser Scanning Confocal Microscope.

184

185 **Figure 1. Biolistics method overview.** Healthy *A. agrestis* thallus tissue, grown on AG medium containing
186 0.2% sucrose, is collected and homogenized. Tissue is washed, filtered, and placed in a 2.5 cm diameter
187 circle onto AG medium containing 2% sucrose. The tissue was allowed to recover for 7 days both before
188 and after transformation. The tissue is pooled from all replicates, homogenized again and placed onto
189 filter paper on AG medium containing 0.2% sucrose to recover for 3 days. For antibiotics selection, tissue
190 is transferred to AG medium, containing 0. 2% sucrose and 10 mg/L hygromycin. Transformed thallus
191 tissue is visible approximately 8-10 weeks after transformation.

192

193

194

195 ***Genome sequencing and transgene copy number estimation***

196 A total of 12 stable lines (four per experiment) were shotgun sequenced to infer transgene copy number.
197 *A. agrestis* thallus tissue was flash-frozen with liquid nitrogen and ground to a fine powder using a mortar
198 and pestle. DNA was extracted using the CTAB protocol described in Li et al. (2020). Illumina library
199 preparation and paired-end sequencing (150 bp), with 50X coverage, was performed by Novogene Corp.
200 Read trimming and quality check were done using fastp v0.23.3 (Chen et al., 2018). We estimated
201 transgene copy number by calculating the median read depth ratio between the *35S* promoter:GFP
202 sequence and single-copy genes in the genome. Using Benchmarking Universal Single-Copy Orthologs
203 (BUSCO; v5.4.7) (Manni et al., 2021), we selected 375 single-copy genes (Supp. Table 1) from *A. agrestis*
204 for read-depth comparison. BWA (v0.7.17) (Li & Durbin, 2009) and SAMtools (v1.17) (Danecek et al., 2021)
205 were used to map reads and calculate read depth, respectively, for the BUSCO genes and the transgene.
206 The command lines and program parameters can be found on figshare (10.6084/m9.figshare.24243559).

207

208 ***Transformation of additional hornwort species***

209 To test the applicability of our method in other hornworts, we selected nine species spanning seven
210 genera and all of the five hornwort families (*Anthoceros fusiformis, Anthoceros punctatus, Anthoceros*
211 *tuberculatus, Leiosporoceros dussii, Megaceros flagellaris, Notothylas orbicularis, Phaeoceros* sp.*,*
212 *Phaeomegaceros chiloensis* and *Phymatoceros phymatodes*). Cultures were maintained as described
213 earlier. Transformation of these species followed the same method used for *A. agrestis*, using the Aa049
214 construct.

215

216 ***Fluorescent protein-tagging and transformation***

217 The *Rubisco small subunit* (*RbcS*, AagrOXF_evm.model.utg000008l.255.1) and *Rubisco activase* (*RCA*,
218 AagrOXF_evm.model.utg000011l.50.1) CDS were identified in the *A. agrestis* genome (Li et al., 2020) using
219 Orthofinder (v2.5.4) (Emms & Kelly, 2019). In the case of *RbcS*, multiple copies of the gene were present,
220 so a copy that showed consistently high expression across multiple conditions was selected to ensure that
221 it was a functional isoform (Li et al., 2020). DNA sequences were synthesized by Twist Biosciences and
222 cloned into L1 vectors. *RCA*, tagged with the *mVenus* fluorescent protein, which was under the control of

223 the *EF1*α and had a *NoS* terminator. *RbcS,* tagged with *mScarlet-I,* was under the control of the *A. agrestis*
224 *RbcS* promoter and also had a *NoS* terminator. The L1 construct was combined with the *Ef1α:hpt:NoS*
225 construct in the *pCSA* L2 vector. Plasmid maps and sequences can be found on figshare
226 (10.6084/m9.figshare.24243559). A*. agrestis* transient and stable transformation followed the method
227 described earlier.

228

229 **Results**

230 ***Efficient transient transformation by biolistics***

231 After conducting experiments to refine the biolistics method for *A. agrestis*, it was determined that the
232 optimal method parameters encompassed the use of 1 µm gold particles, a helium pressure of 600 psi, a
233 vacuum pressure of 28 inHg, and a bombardment plate distance of 14 cm from the source. These
234 parameters were chosen for future experiments because more severe tissue damage was observed when
235 bombarding at higher pressures and shorter plate distances. To quantify the number of cells transiently
236 expressing GFP, we developed an efficient semi-automatic procedure using CellProfiler (Stirling et al.,
237 2021). This method has previously been used to quantify the transient transformation efficiency in
238 biolistically transformed onion and *Nicotiana benthamiana* (Miller et al., 2021). We confirmed the results
239 from CellProfiler with manual counting and found a strong linear correlation, with a Pearson correlation
240 coefficient (r) of 0.98 (Supp. Fig. 1).

241 To assess the efficacy and reproducibility of transient transformation, five separate experiments (with 10
242 replicates each) were performed (Fig. 2C). Across all successfully transformed replicates, there was an
243 average of 569 (± 268) transiently expressing GFP cells from one bombardment experiment. These results
244 were quantified 72 hours after transformation, with fluorescence first observed within 24 hours. We
245 found high variability between replicates in each experiment, for example in experiment 1, one replicate
246 had 1158 transiently expressing cells while another had 114. This variability was reduced when comparing
247 the means from each experiment, which ranged from 474 to 701 transient events (Fig. 2). In addition, not
248 all replicates were successfully transformed (i.e. no GFP signal observed from any cell). These were
249 removed from downstream analysis (2-4 per experiment; Fig. 2). It is unknown what caused
250 inconsistencies, with potential factors being poor tissue health, tissue moisture level or aggregation of
251 gold particles on the macrocarrier, all of which can reduce transformation efficiency (Southgate et al.,
252 1995).

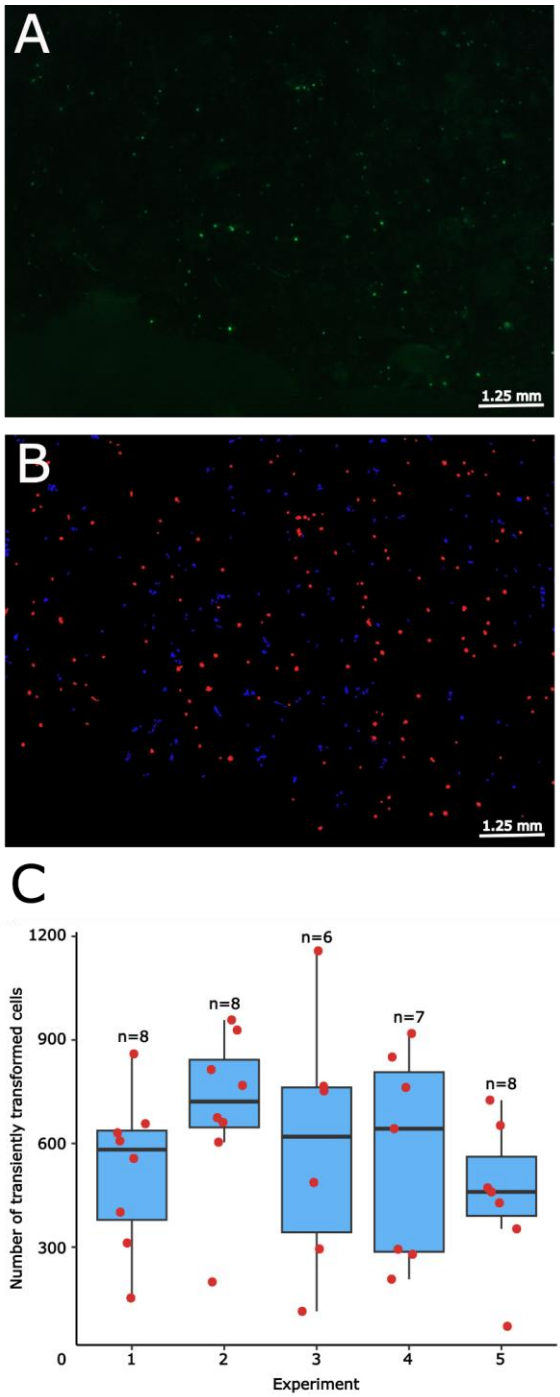

Figure 2. Transient transformation of *Anthoceros agrestis* and event quantification. (A) The unprocessed image of tissue transiently expressing GFP, taken with a Leica M205 stereomicroscope. (B) The same image in A after processing with CellProfiler, where blue signals represent artifact objects or cells/tissue not expressing GFP and red signals are transformed cells expressing GFP. (C) Boxplot displaying the number of cells transiently expressing GFP, across five separate experiments. Individual replicates are plotted as red dots. The box represents the 25th and 75th percentile, with the horizontal line being the median value and the vertical lines marking the minimum and maximum, excluding outliers.

260 ***Recovery of stable transformants***

261 Although transient transformation resulted in hundreds of transient events, it was initially challenging to
262 recover stably transformed lines. In our earlier attempts, we allowed the bombarded tissue to recover for
263 7 days before cutting into 2 mm^2 pieces and transferring to AG medium containing 0.2% sucrose and
264 10 mg/L hygromycin. Over the following weeks, we observed that GFP-expressing tissue persisted,
265 however, the surrounding tissue also survived much longer than other non-transformed tissue. HPT
266 inactivates hygromycin via phosphorylation (Rao et al., 1983) and in *Arabidopsis*, HPT was shown to be
267 secreted into the extracellular space (Zhang et al., 2011). It is possible that hygromycin is inactivated in
268 the medium surrounding transformed tissue, allowing untransformed tissue to 'feed' off it, limiting
269 regeneration. To overcome this, tissue was homogenized before being placed on selection medium in
270 order to reduce the amount of non-transformed tissue surrounding the transformed tissue. After 8-10
271 weeks of selection, the first regenerating hygromycin-resistant thallus tissue was visible and were
272 transferred to fresh selection medium for propagation. The presence of the transgene was confirmed via
273 fluorescent microscopy and PCR, with primers designed to span the *Ef1α* promoter and *hpt* CDS (Supp.
274 Fig. 2-4). This was repeated across three separate experiments, with five replicates in experiments 1 and
275 2, and four replicates in experiment 3. These experiments regenerated 20, 49 and 12 individual lines,
276 respectively, totaling 81 lines. On average, each bombardment of 0.2 g of tissue yielded six stable
277 transformants.

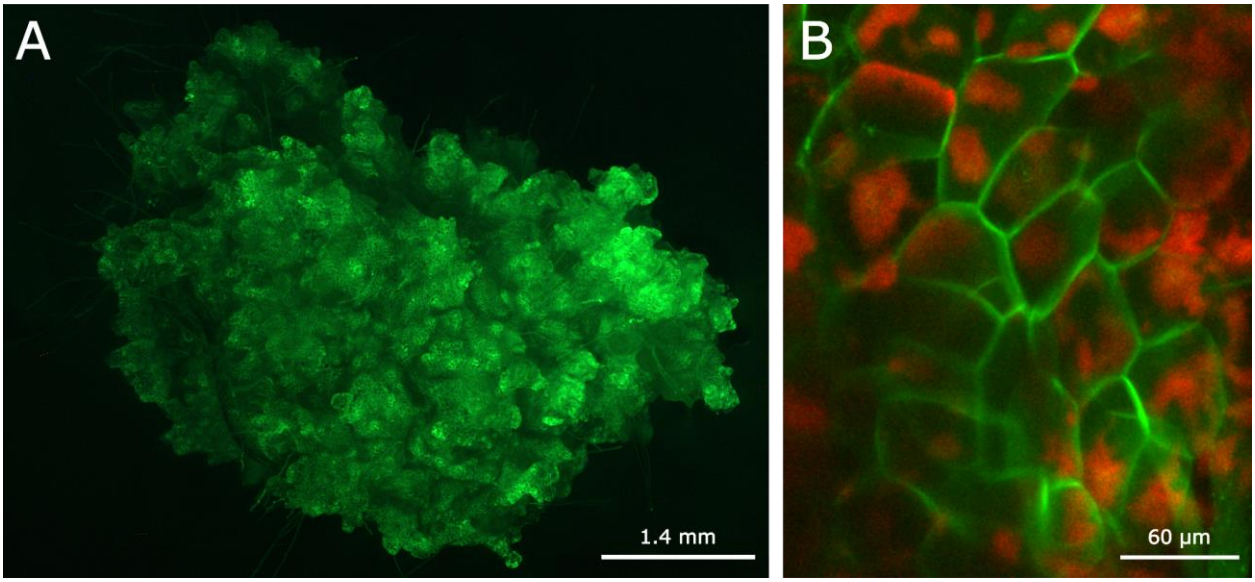

278 **Figure 3. Stable transformation of *Anthoceros agrestis*.** Transformed thallus expressing membrane-
279 localized GFP was imaged using (A) a Leica M205 stereomicroscope, with the GFP channel, and (B) a Leica

280 TCS SP5 Laser Scanning Confocal Microscope, showing both chlorophyll autofluorescence in red and GFP
281 signal in green.

282 A drawback of biolistics-mediated transformation is the potential for high transgene copy number, which
283 may lead to instability and potential gene silencing (Kohli et al., 2003). To assess the transgene copy
284 number, we shotgun sequenced four stable lines per experiment, and compared the median read depth
285 of the *35Spro:GFP* sequence to the median read depth for a set of single-copy genes (here the BUSCO
286 genes were used; Table 1, Supp. Table 1). The whole plasmid was not used for read depth comparison as
287 it contained the native hornwort Ef1a promoter and multiple copies of the NOS terminator. We found
288 that 50% of the sequenced lines had a copy number fewer than four, and 30% had a single copy. Several
289 lines had very large copy numbers, with the highest estimated at 75.

290

291 **Table 1. Transgene copy number estimate for the sequenced stable lines.** Note that although two lines
292 had a BUSCO-GFP ratio of less than 1, GFP expression was still observed and there was even read coverage
293 across the entire GFP cassette with no missing sequences.

	Line	BUSCO Median Read Depth	GFP Cassette Median Read Depth	BUSCO-GFP Ratio	Inferred copy number
Experiment 1	1a	53	370	6.98	7
	1b	41	552	13.46	13
	1c	53	1552	29.28	29
	1d	42	23	0.55	1
Experiment 2	2a	50	50	1.00	1
	2b	67	133	1.99	2
	2c	58	45	0.78	1
	2d	74	5541	74.88	75
Experiment 3	3a	48	153	3.19	3
	3b	44	45	1.02	1
	3c	28	1826	65.21	65
	3d	42	422	10.05	10

294

295 ***Broad applicability to other hornwort species***

296 To assess the applicability of the biolistics method to other hornwort species, we tested a total of nine
297 species spanning the entire hornwort phylogeny: *Anthoceros fusiformis, Anthoceros punctatus,*
298 *Anthoceros tuberculatus, Leiosporoceros dussii, Megaceros flagellaris, Notothylas orbicularis, Phaeoceros*
299 sp.*, Phaeomegaceros chiloensis* and *Phymatoceros phymatodes*. The majority of species had fewer

transiently expressing GFP cells than *A. agrestis*, while both *A. punctatus* and *N. orbicularis* had a greater number (Fig. 4). Stable transformants were obtained for *A. fusiformis* with 29 lines recovered from one experiment (Supplementary Fig. 5). The method will need to be optimized for each species in order to increase the efficiency of transient transformation and to obtain stable transformants.

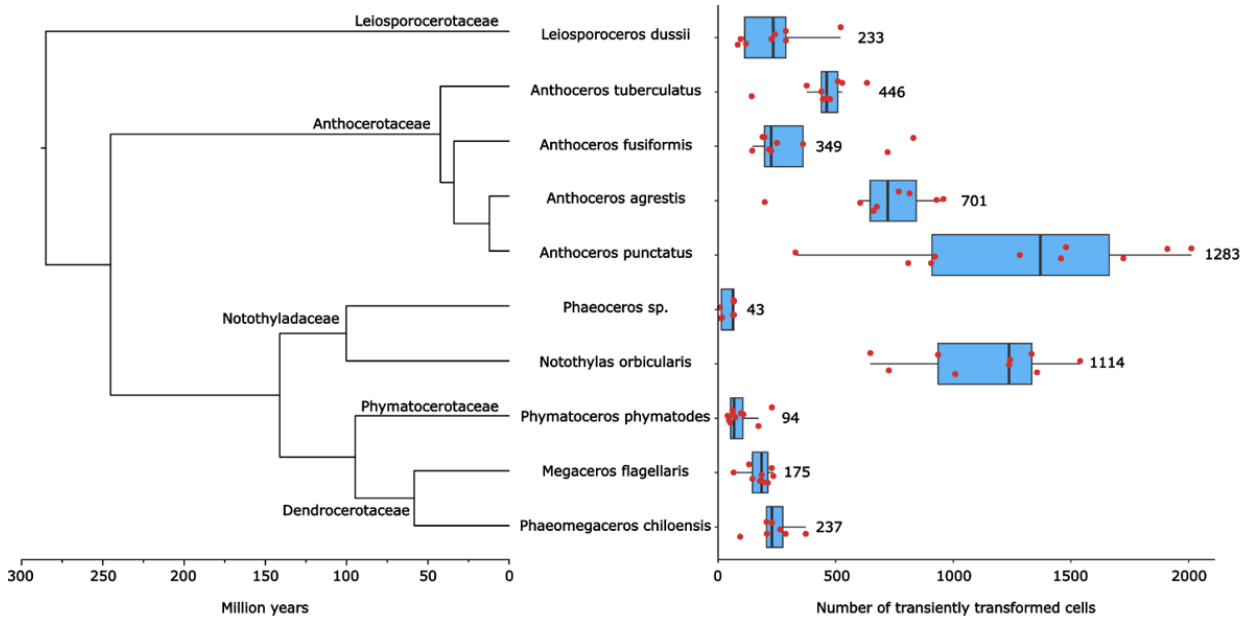

Figure 4. Transient transformation of hornwort species across the phylogeny. Our method can be directly applied to generate transient transformants in species covering all hornwort families and most of the genera. Phylogenetic tree displays timing of divergence, adapted from Bechteler et al. (2023). Red dots represent the value of replicates and numbers represent the average number of transiently transformed cells per bombardment. The box represents the 25th and 75th percentile, with the vertical line being the median value. The horizontal lines represent the minimum and maximum, excluding outliers.

Transient and stable expression of fluorescently tagged Rubisco and Rubisco activase

To demonstrate the applicability of the biolistics-mediated transformation method for hornwort studies, we used it to investigate the structure of hornwort pyrenoids by localizing two putative pyrenoid-containing proteins, the Rubisco small subunit (RbcS) and Rubisco activase (RCA) through co-transformation of *A. agrestis*. The *RbcS* coding sequence was fused to the mScarlet-I fluorophore and the *RCA* coding sequence was fused to the mVenus fluorophore. Co-transformation of these two constructs clearly showed that RbcS and RCA co-localized, with fluorescence tightly confined within round structures

320 in the chloroplast corresponding to hornwort pyrenoids (Fig. 5). Pyrenoids appear as distinct black holes
321 under the chlorophyll autofluorescence channel, which is consistent with the early ultrastructural studies
322 based on transmission electron microscopy (Vaughn et al., 1992). Furthermore, we obtained stably
323 transformed lines expressing either the RbcS:msScarlet-I or the RCA:mVenus constructs. Again, the
324 fluorescence signals were highly concentrated in pyrenoid structures that are devoid of chlorophyll
325 autofluorescence.

326

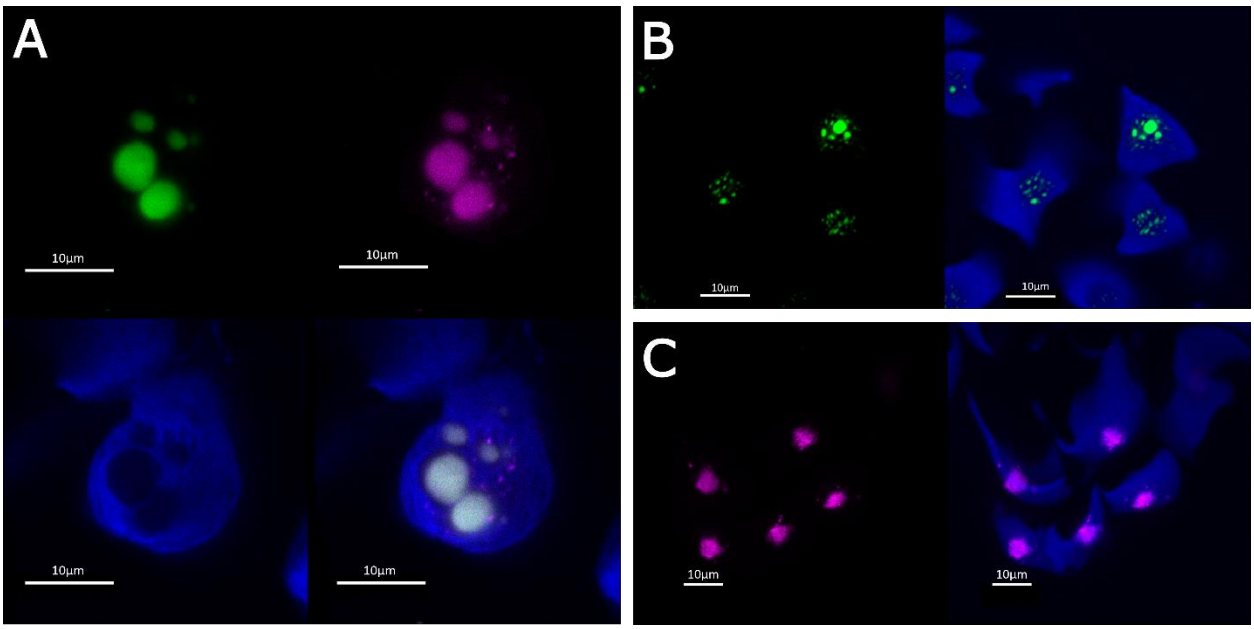

327 **Figure 5. Transient and stable transformation of pyrenoid-related genes in *Anthoceros agrestis*.** (A) *A.*
328 *agrestis* thallus tissue was co-transformed with *RbcS:mScarlet-I* and *RCA:mVenus* constructs. The pyrenoid
329 regions lack chlorophyll autofluorescence (blue) and are instead packed with tagged RbcS and RCA. The
330 overlapping mScarlet-I and mVenus fluorescence signal strongly suggests co-localization of RbcS and RCA
331 to pyrenoids. *A. agrestis* thallus tissue stably expressing (B) *RCA:mVenus* and (C) *RbcS:mScarlet-I*, with
332 chlorophyll in blue. All images were taken using a Leica TCS SP5 Laser Scanning Confocal Microscope.

333

334

335

336

337

338

339

340

341 **Discussion**

342 ***A biolistics method for transient and stable transformation across the hornwort phylogeny***

343 Our current method resulted in a high number of transient and stable events for *A. agrestis*. From 0.2 g
344 of bombarded tissue, we obtained on average 569 (± 268) transiently transformed cells and six stable
345 insertion lines. Furthermore, we provide the first account of transient transformation in *A. tuberculatus,*
346 *M. flagellaris, N. orbicularis, Phaeoceros* sp*., Phaeomegaceros chiloensis* and *Phymatoceros phymatodes*,
347 together covering all the hornwort families. It is important to note that these hornwort species are deeply
348 diverged; they share the most recent common ancestor almost 300 million years ago (Bechteler et al.,
349 2023), which predates the origin of flowering plants (Ramírez-Barahona et al., 2020). The successful
350 transient transformation of multiple hornwort species suggests that our method is widely applicable
351 across taxa, thus broadening the scope of genetic manipulation in hornworts. The ability to transform
352 diverse hornwort species enables comparative studies to identify conserved genetic elements, especially
353 for convergently evolved traits. For example, pyrenoids have originated independently approximately five
354 to six times during hornwort evolution, resulting in vastly different morphologies and CCM strength across
355 species (Vaughn et al., 1990; Hanson et al., 2002; Villarreal & Renner, 2012; Li et al., 2017). Understanding
356 the genetic basis of such repeated evolution could have important implications in engineering CCMs in
357 other plants. Likewise, U/V sex chromosomes have experienced multiple gains and losses in hornworts
358 (Villarreal & Renner, 2013). Future work could use our biolistics method to test if similar genetic elements
359 have been convergently recruited to sex chromosomes.

360 Despite the relatively high number of transient events, we had mixed success in generating stable
361 transformants from diverse hornwort species. While 29 *A. fusiformis* stable lines were recovered from
362 one experiment, we did not recover stable events from the remaining species. It is likely that the method
363 will need to be optimized for each species. In particular, we have observed that a number of species have
364 a slower growth rate on AG medium, which indicates that the post homogenization recovery time may
365 need to be extended. In our constructs, the *A. agrestis Ef1α* promoter drives *hpt* expression, however, it
366 is possible that this promoter may not function well in other hornwort species, especially considering the
367 timing of divergence (Fig. 4), and their native *Ef1a* promoter is required. The optimal antibiotic
368 concentration to select for transgenic events may also vary between species.

369

370

371 ***Relative high frequency of low transgene copy number in stably transformed lines***

372 A common issue for biolistics-mediated transformation is the possibility of multiple transgene insertions
373 into the genome. Here we report that 33% of sequenced transgenic lines were estimated to have single-
374 copy insertions, and 50% of the lines have less than four copies. The frequency of low-copy insertions is
375 much higher when compared to biolistics transformation of other bryophytes. Studies in the liverwort
376 *Marchantia polymorpha* and the moss *Physcomitrium patens* found that only 10% of regenerated lines
377 had single copies of the transgene (Irifune et al., 1996; Šmídková et al., 2010). Nevertheless, we did
378 occasionally observe lines with a large transgene copy number, with two lines having an estimated 63 and
379 73 copies, respectively. While *Agrobacterium*-mediated transformation of hornworts has been
380 demonstrated, the frequency of low copy number events was not reported (Frangedakis et al., 2021b,
381 Waller et al., 2023). It is likely that the frequency of single-copy insertions can be further increased using
382 a minimal cassette, where the genes of interest are amplified using PCR, eliminating the backbone from
383 transformation. This technique typically requires less DNA for transformation. Two studies in wheat aimed
384 to increase the number of single copy events by using minimal cassettes, resulting in an average of 38%
385 and 50% of single-copy insertions (Tassy et al., 2014; Ismagul et al., 2018), while in rice 80% of regenerated
386 lines were estimated to have less than two transgene copies (Fu et al., 2000).

387

388 ***Using fluorescent protein tagging to visualize hornwort pyrenoids***

389 Application of this method enabled us to observe localization of fluorescently tagged proteins within 48
390 hours post bombardment and nine days from the point the tissue was first homogenized. The biolistics
391 method thus provides the ability to quickly assess protein function, localization, and interactions without
392 the need to generate stable transformants. We demonstrated that our method can be used to study
393 proteins associated with pyrenoids and CCM function.

394 Pyrenoids are membraneless micro-compartments within the chloroplasts of algae and hornworts that
395 are composed predominantly of Rubisco. This aggregation of Rubisco enables the function of a biophysical
396 CCM providing a central locus in which to concentrate CO_2. While pyrenoids are present in many algal
397 species and have been extensively studied in the model alga *Chlamydomonas reinhardtii* (He et al., 2023),
398 hornworts are the only land plants with pyrenoids and have received little research attention (Li et al.,
399 2017). Early ultrastructural studies reported that hornwort pyrenoids are tightly sandwiched by thylakoids

400 (as opposed to starch sheaths in algae) (Burr, 1970; Vaughn et al., 1992), and based on immunogold
401 labeling are indeed the locations where Rubisco are concentrated (Vaughn et al., 1990). We set out to
402 visualize pyrenoids by fluorescent protein tagging and to establish pyrenoid marker proteins for future
403 studies. To this end, we focused on the Rubisco small subunit (RbcS) as well as Rubisco activase (RCA),
404 which is required for Rubisco activation and activity maintenance (McKay et al., 1991). In *C. reinhardtii*
405 both proteins are known to localize predominantly in pyrenoids (Mackinder et al., 2017). We co-
406 transformed RbcS and RCA tagged with the mScarlet-I and mVenus fluorescent protein, respectively, into
407 *A. agrestis* thalli. RbcS and RCA were found to clearly co-localize to pyrenoids based on the overlapping
408 mScarlet-I and mVenus signals (Fig. 5). To our knowledge, this is the first application of genetic engineering
409 to interrogate gene function in hornworts. Importantly, it is now possible to use either fluorescently
410 tagged RbcS or RCA as a pyrenoid marker, and co-transform it with candidate genes to build a spatial
411 protein localization model for hornwort CCMs. Furthermore, we show the successful regeneration of lines
412 stably expressing either *RbcS:mScarlet-I* or *RCA:mVenus*. Currently, these transformants are being used to
413 track pyrenoid development and to understand how it is impacted by environmental factors such as CO_2
414 concentration.

415 In conclusion, we report the first biolistics protocol for transformation of a phylodiverse set of hornwort
416 species, as well as the first gene functional study in the model hornwort *Anthoceros agrestis*. We
417 anticipate our work to allow new avenues for investigation and biotechnological applications, such as
418 genome editing. The achievement of both stable and transient transformation provides powerful tools for
419 studying gene function in hornworts. These advances lay the foundation for future research aimed at
420 unraveling the mysteries of hornwort biology and harnessing their unique characteristics for sustainable
421 agriculture.

422

423 **Supplemental Data**

424 Supplemental Table 1. BUSCO genes used in transgene copy number estimation analysis.

425 Supplemental Figure 1. Correlation between manual and CellProfiler counting of cells transiently
426 expressing GFP.

427 Supplemental Figure 2. *Anthoceros agrestis* stable lines regenerated from experiment 1.

428 Supplemental Figure 3. *Anthoceros agrestis* stable lines regenerated from experiment 2.

429 Supplemental Figure 4. *Anthoceros agrestis* stable lines regenerated from experiment 3.

430 Supplemental Figure 5. *Anthoceros fusiformis* stable lines.

431 **Acknowledgements**

432 We thank Eftychis Frangedakis for providing the materials in the OpenPlant toolkit and transformation
433 advice, Peter Schafran for helping with estimating transgene copy numbers, Mamta Srivastava for helping
434 with confocal and fluorescence microscopy and Jenna Sins and Evan Smith for laboratory assistance.

435

436 **Author contributions**

437 FWL and JVE: conceptualization; DL: formal analysis; FWL, JVE, and LHG: funding acquisition; DL, TAR, and
438 AG: investigation; DL and AG: methodology; FWL, JVE, and LHG: supervision; DL and TAR: visualization; DL
439 and FWL: writing—original draft.

440

441 **Conflict of interest**

442 None declared.

443

444 **Funding**

445 NSF IOS 1923011 to FWL and JVE, and NSF MCB 2213841 to FWL and LHG.

446

447 **Data availability**

448 The raw Illumina reads for quantifying transgene copy numbers were deposited in NCBI SRA (under the
449 BioProject PRJNA1029596).

450

451

452

453

References

Adler L, Díaz-Ramos A, Mao Y, Pukacz KR, Fei C, McCormick AJ. 2022. New horizons for building pyrenoid-based CO2-concentrating mechanisms in plants to improve yields. *Plant Physiology* 190, 1609–1627.

Atkinson N, Mao Y, Chan KX, McCormick AJ. 2020. Condensation of Rubisco into a proto-pyrenoid in higher plant chloroplasts. *Nature Communications* 11, 6303.

Blechteler J, Gabriel Peñaloza-Bojacá G, Bell D, *et al*. 2023. Comprehensive phylogenomic time tree of bryophytes reveals deep relationships and uncovers gene incongruences in the last 500 million years of diversification. *American Journal of Botany* in press. Doi: 10.1002/ajb2.16249.

Burr FA. 1970. Phylogenetic transitions in the chloroplasts of the Anthocerotales. I. The number and ultrastructure of the mature plastids. *American Journal of Botany* 57, 97–110.

Chatterjee P, Schafran P, Li F-W, Meeks JC. 2022. Nostoc talks back: Temporal patterns of differential gene expression during establishment of *Anthoceros-Nostoc* symbiosis. *Molecular Plant-Microbe Interactions* 35, 917-932.

Chen S, Zhou Y, Chen Y, Gu J. 2018. fastp: an ultra-fast all-in-one FASTQ preprocessor. *Bioinformatics* 34, 884-890.

Danecek P, Bonfield JK, Liddle J, *et al*. 2021. Twelve years of SAMtools and BCFtools. *GigaScience* 10, doi: 10.1093/gigascience/giab008

Emms DM, Kelly S. 2019. OrthoFinder: phylogenetic orthology inference for comparative genomics. *Genome Biology* 20, 1-14

Frangedakis E, Shimamura M, Villarreal JC, Li F-W, Tomaselli M, Waller M, Sakakibara K, Renzaglia KS, Szövényi P. 2021a. The hornworts: morphology, evolution and development. *The New Phytologist* 229, 735–754.

Frangedakis E, Waller M, Nishiyama T, *et al*. 2021b. An Agrobacterium-mediated stable transformation technique for the hornwort model *Anthoceros agrestis*. *The New Phytologist* 232, 1488–1505.

Fu X, Duc LT, Fontana S, Bong BB, Tinjuangjun P, Sudhakar D, Twyman RM, Christou P, Kohli A. 2000. Linear transgene constructs lacking vector backbone sequences generate low-copy-number transgenic plants with simple integration patterns. *Transgenic Research* 9, 11–19.

Gunadi A, Li F-W, Van Eck J. 2022. Accelerating gametophytic growth in the model hornwort *Anthoceros agrestis*. *Applications in Plant Sciences* 10, e11460.

Hanson D, Andrews TJ, Badger MR. 2002. Variability of the pyrenoid-based CO_2 concentrating mechanism in hornworts (Anthocerotophyta). *Functional Plant Biology* 29, 407–416.

He S, Crans VL, Jonikas MC. 2023. The pyrenoid: the eukaryotic CO2-concentrating organelle. *The Plant Cell* 35, 3236–3259.

Irifune K, Ono K, Takahashi M, Murakami H, Morikawa H. 1996. Stable transformation of cultured cells of the liverwort *Marchantia polymorpha* by particle bombardment. *Transgenic Research* 5, 337–341.

Ismagul A, Yang N, Maltseva E, *et al*. 2018. A biolistic method for high-throughput production of transgenic wheat plants with single gene insertions. *BMC Plant Biology* 18, 135.

Kohli A, Twyman RM, Abranches R, Wegel E, Stoger E, Christou P. 2003. Transgene integration, organization and interaction in plants. *Plant Molecular Biology* 52, 247–258.

Lacroix B, Citovsky V. 2020. Biolistic approach for transient gene expression studies in plants. *Methods in Molecular Biology* 2124, 125–139.

Li F-W, Nishiyama T, Waller M, *et al.* 2020. *Anthoceros* genomes illuminate the origin of land plants and the unique biology of hornworts. *Nature Plants* 6, 259–272.

Li F-W, Villarreal JC, Szövényi P. 2017. Hornworts: An overlooked window into carbon-concentrating mechanisms. *Trends in Plant Science* 22, 275–277.

Li H, Durbin R. 2009. Fast and accurate short read alignment with Burrows–Wheeler transform. *Bioinformatics* 25, 1754–1760.

Mackinder LCM, Chen C, Leib RD, Patena W, Blum SR, Rodman M, Ramundo S, Adams CM, Jonikas MC. 2017. A spatial interactome reveals the protein organization of the algal CO2-concentrating mechanism. *Cell* 171, 133-147.

Manni M, Berkeley MR, Seppey M, Simão FA, Zdobnov EM. 2021. BUSCO update: Novel and streamlined workflows along with broader and deeper phylogenetic coverage for scoring of eukaryotic, prokaryotic, and viral genomes. *Molecular Biology and Evolution* 38, 4647–4654.

Martin-Ortigosa S, Wang K. 2014. Proteolistics: a biolistic method for intracellular delivery of proteins. *Transgenic Research* 23, 743–756.

McKay RML, Gibbs SP, Vaughn KC. 1991. RuBisCo activase is present in the pyrenoid of green algae. *Protoplasma* 162, 38–45.

Meeks JC. 1998. Symbiosis between nitrogen-fixing cyanobacteria and plants. *Bioscience* 48, 266–276.

Meyer MT, McCormick AJ, Griffiths H. 2016. Will an algal CO2-concentrating mechanism work in higher plants? *Current Opinion in Plant Biology* 31, 181–188.

Miller K, Eggenberger AL, Lee K, Liu F, Kang M, Drent M, Ruba A, Kirscht T, Wang K, Jiang S. 2021. An improved biolistic delivery and analysis method for evaluation of DNA and CRISPR-Cas delivery efficacy in plant tissue. *Scientific Reports* 11, 7695.

Morris JL, Puttick MN, Clark JW, Edwards D, Kenrick P, Pressel S, Wellman CH, Yang Z, Schneider H, Donoghue PCJ. 2018. The timescale of early land plant evolution. *Proceedings of the National Academy of Sciences of the United States of America* 115, E2274–E2283.

Nelson JM, Hauser DA, Li F-W. 2021. The diversity and community structure of symbiotic cyanobacteria in hornworts inferred from long-read amplicon sequencing. *American Journal of Botany* 108, 1731-1744.

Neubauer A, Ruaud S, Waller M, Frangedakis E, Li F-W, Nötzold SI, Wicke S, Bailly A, Szövényi P. 2022. Step-by-step protocol for the isolation and transient transformation of hornwort protoplasts. *Applications in Plant Sciences* 10, e11456.

Ramírez-Barahona S, Sauquet H, Magallón S. 2020. The delayed and geographically heterogeneous diversification of flowering plant families. *Nature Ecology and Evolution* 4: 1232–1238.

Rao RN, Allen NE, Hobbs JN Jr, Alborn WE Jr, Kirst HA, Paschal JW. 1983. Genetic and enzymatic basis of hygromycin B resistance in *Escherichia coli*. *Antimicrobial Agents and Chemotherapy* 24, 689–695.

Sanford JC, Klein TM, Wolf ED, Allen N. 1987. Delivery of substances into cells and tissues using a particle bombardment process. *Particulate Science and Technology* 5, 27–37.

Sauret-Güeto S, Frangedakis E, Silvestri L, Rebmann M, Tomaselli M, Markel K, Delmans M, West A, Patron NJ, Haseloff J. 2020. Systematic tools for reprogramming plant gene expression in a simple model, *Marchantia polymorpha*. *ACS Synthetic Biology* 9, 864–882.

Šmídková M, Holá M, Angelis KJ. 2010. Efficient biolistic transformation of the moss *Physcomitrella patens*. *Biologia Plantarum* 54, 777–780.

Southgate EM, Davey MR, Power JB, Marchant R. 1995. Factors affecting the genetic engineering of plants by microprojectile bombardment. *Biotechnology Advances* 13, 631–651.

Stirling DR, Swain-Bowden MJ, Lucas AM, Carpenter AE, Cimini BA, Goodman A. 2021. CellProfiler 4: improvements in speed, utility and usability. *BMC Bioinformatics* 22, 433.

Svitashev S, Schwartz C, Lenderts B, Young JK, Mark Cigan A. 2016. Genome editing in maize directed by CRISPR–Cas9 ribonucleoprotein complexes. *Nature Communications* 7, 1–7.

Szövényi P, Frangedakis E, Ricca M, Quandt D, Wicke S, Langdale JA. 2015. Establishment of *Anthoceros agrestis* as a model species for studying the biology of hornworts. *BMC Plant Biology* 15, 98.

Tassy C, Partier A, Beckert M, Feuillet C, Barret P. 2014. Biolistic transformation of wheat: increased production of plants with simple insertions and heritable transgene expression. *Plant Cell, Tissue and Organ Culture* 119, 171–181.

Vaughn KC, Campbell EO, Hasegawa J, Owen HA, Renzaglia KS. 1990. The pyrenoid is the site of ribulose 1,5-bisphosphate carboxylase/oxygenase accumulation in the hornwort (Bryophyta: Anthocerotae) chloroplast. *Protoplasma* 156, 117–129.

Vaughn KC, Ligrone R, Owen HA, Hasegawa J, Campbell EO, Renzaglia KS, Monge-Najera J. 1992. The anthocerote chloroplast: a review. *The New Phytologist* 120, 169–190.

Villarreal JC, Renner SS. 2013. Correlates of monoicy and dioicy in hornworts, the apparent sister group to vascular plants. *BMC Evolutionary Biology* 13, 239.

Villarreal JC, Renner SS. 2012. Hornwort pyrenoids, carbon-concentrating structures, evolved and were lost at least five times during the last 100 million years. *Proceedings of the National Academy of Sciences of the United States of America* 109, 18873–18878.

Waller M, Frangedakis E, Marron AO, Sauret-Gueto S, Rever J, Sabbagh CRR, Hibberd JM, Haseloff J, Renzaglia K, Szövényi, P. 2023. An optimised transformation protocol for *Anthoceros agrestis* and three more hornwort species. *The Plant Journal* 114, 699-718

Zhang H, Zhang L, Gao B, Fan H, Jin J, Botella MA, Jiang L, Lin J. 2011. Golgi apparatus-localized synaptotagmin 2 is required for unconventional secretion in *Arabidopsis*. *PloS One* 6, e26477.

Zhang Y, Liang Z, Zong Y, Wang Y, Liu J, Chen K, Qiu J-L, Gao C. 2016. Efficient and transgene-free genome editing in wheat through transient expression of CRISPR/Cas9 DNA or RNA. *Nature Communications* 7, 12617.

Homogenize
2.5 cm
7-day
recovery
Bombardment
7-day recovery then
homogenize
To selection
after 3 days
On
selection
for 8 weeks

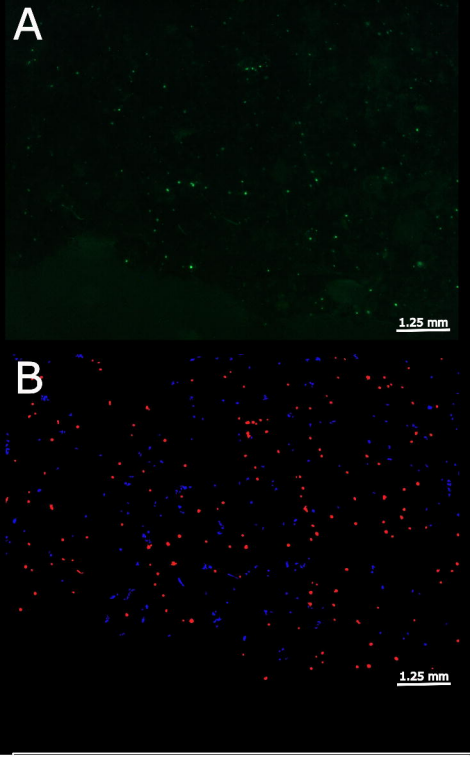
A
1.25 mm
B
1.25 mm

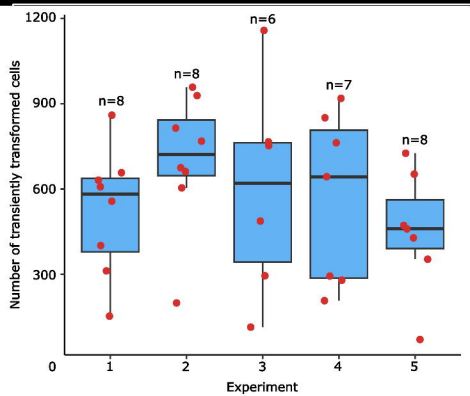
1200
900
600
300
0
Number of transiently transformed cells
n=8
n=8
n=6
n=7
n=8
1
2
3
4
5
Experiment

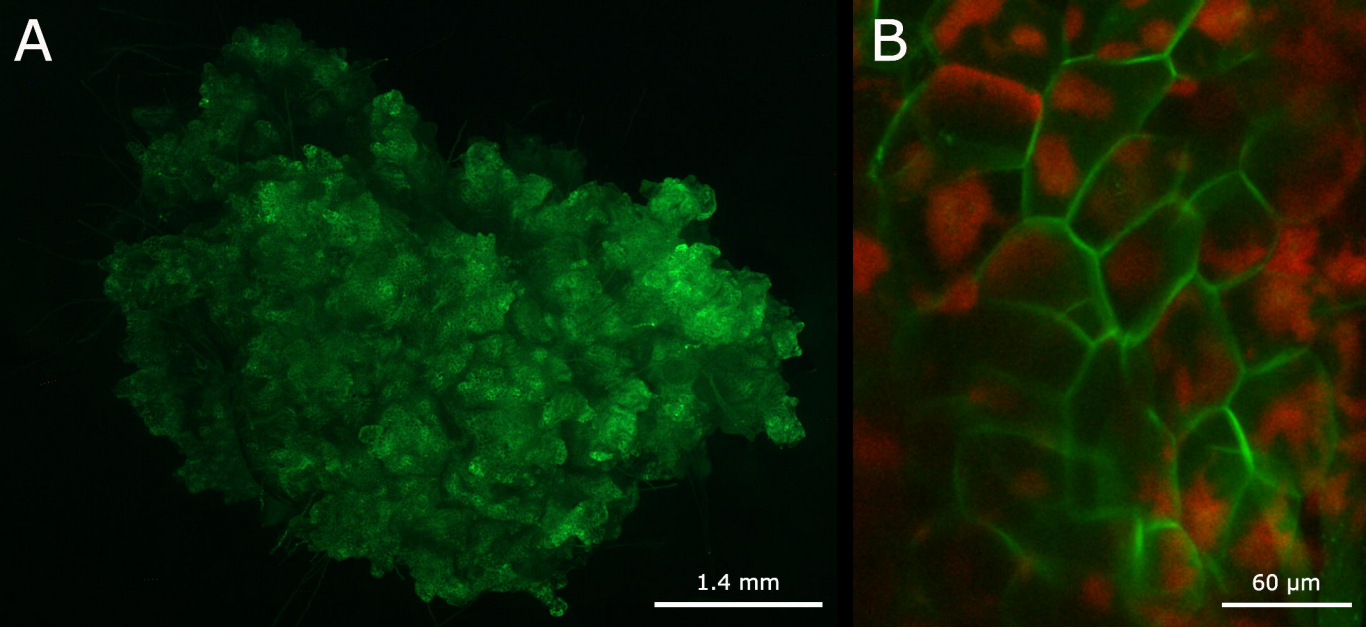
A
1.4 mm
B
60 µm

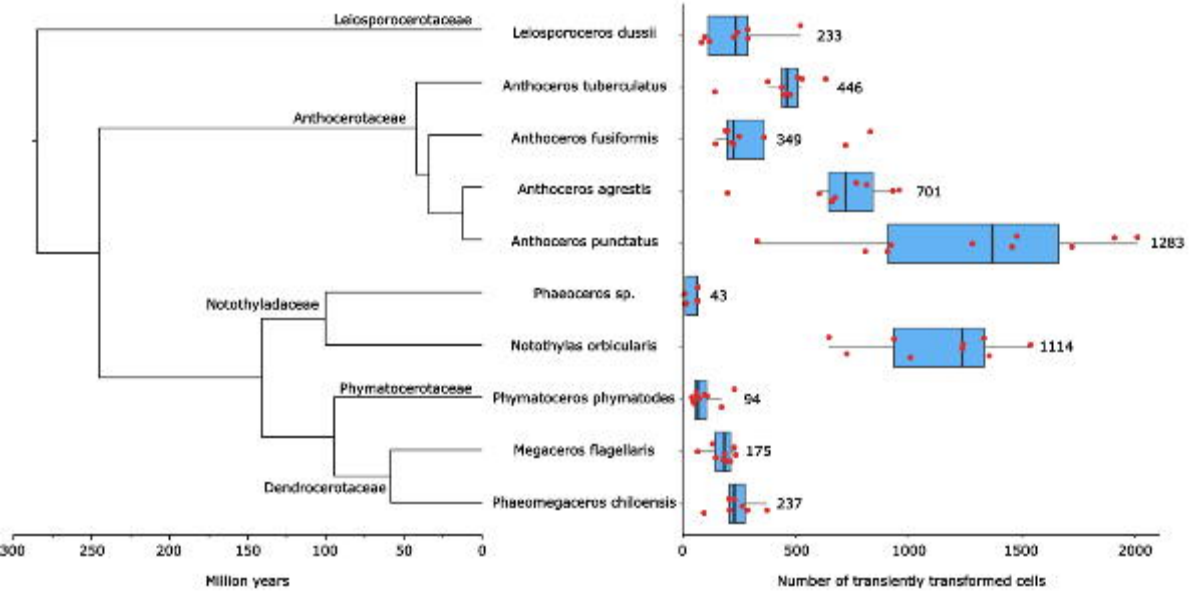
Leiosporocerotaceae
Anthocerotaceae
Notothyladaceae
Phymatocerotaceae
Dendrocerotaceae
Leiosporoceros dussii
Anthoceros tuberculatus
Anthoceros fusiformis
Anthoceros agrestis
Anthoceros punctatus
Phaeoceros sp.
Notothylas orbicularis
Phymatoceros phymatodes
Megaceros flagellaris
Phaeomegaceros chilensis
233
446
349
701
1283
43
1114
94
175
237
300
250
200
150
100
50
0
Million years
0
500
1000
1500
2000
Number of transiently transformed cells

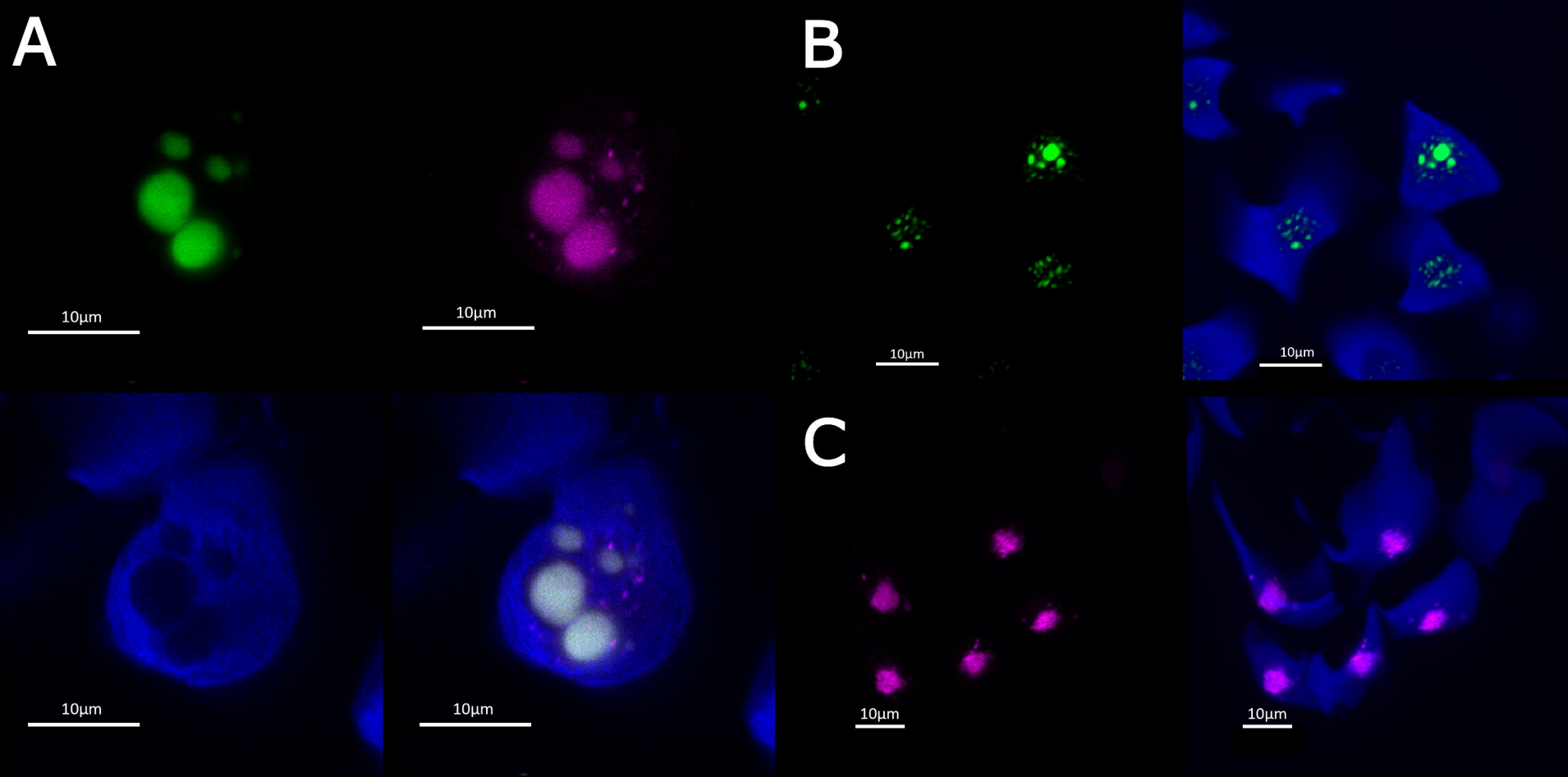
A
10µm
10µm
B
10µm
10µm
10µm
10µm
C
10µm
10µm